1-18-2008

Cross sections for 11–14-eV e-H2 resonant collisions: Vibrational excitation

R Celiberto
Istituto di Metodologie Inorganiche e Plasmi, CNR, Bari, Italy

R. K. Janev
Macedonian Academy of Sciences and Arts, Skopje, Macedonia

J. M. Wadehra
Wayne State University, ad5541@wayne.edu

A Laricchiuta
Istituto di Metodologie Inorganiche e Plasmi, CNR, Bari, Italy

Cross sections for 11–14-eV e-H_2 resonant collisions: Vibrational excitation

R. Celiberto,[1,*] R. K. Janev,[2,†] J. M. Wadehra,[3,‡] and A. Laricchiuta[4,§]
[1]*Department of Water Engineering and Chemistry, Polytechnic of Bari, 70125 Bari, Italy*
[2]*Macedonian Academy of Sciences and Arts, 1000 Skopje, Macedonia*
[3]*Physics Department, Wayne State University, Detroit, Michigan 48202, USA*
[4]*Institute of Inorganic Methodologies and Plasmas, CNR, 70125 Bari, Italy*
(Received 23 April 2007; revised manuscript received 27 October 2007; published 18 January 2008)

Resonant vibrational excitation (RVE) cross sections have been calculated for the *electron*-H_2 molecule collisions in the energy range 11–14 eV involving the $^2\Sigma_g^+$ excited electronic state of the molecular hydrogen ion H_2^-. This state, whose threshold is located around 14 eV, gives rise to the so-called series *a* of the observed peaks in electron-impact differential cross-section measurements. The calculations have been performed within the local complex potential approximation by using the available theoretical potential energy and width for the $^2\Sigma_g^+$ resonant state. The cross sections for all $v_i=0\rightarrow v_f=1-14$ RVE transitions have been calculated. A satisfactory agreement of calculated cross sections with the available experimental data is obtained.

DOI: 10.1103/PhysRevA.77.012714 PACS number(s): 34.80.Ht, 34.50.−s

I. INTRODUCTION

Electron-impact resonant collision processes involving H_2 molecules play a decisive role in some technological application of hydrogen plasmas [1]. Extensive cross-section calculations and measurements have been performed in the past decades for the processes of dissociative electron attachment (DEA) and resonant vibrational excitations (RVE) occurring through the formation of the intermediate negative H_2^- ion in its ground $^2\Sigma_u^+$ state and the lowest $^2\Sigma_g^+$ state. These two states give rise to the well-known 3.75 and 10 eV resonance peaks in the measured DEA cross sections [2]. The underlying mechanisms for these processes have been well-understood and the experimental data have been successfully reproduced by various theoretical models [3,4].

Quite different is the situation with the so-called 14 eV peak observed in the early DEA experiments of Shulz [5] and Rapp *et al.* [6]. The origin of this peak was initially attributed to an asymptotic Rydberg state [6] correlating with the $H(n=2)+H^-(1s^2)$ reaction channel, having a threshold at 13.92 eV [7]. The existence of resonant states in the energy region between 11 and 15 eV has been experimentally observed by many authors [8,9] and conclusively confirmed by Comer and Read [10] and Joyez *et al.* [11], who performed energy loss measurements on H_2 and D_2 molecules, measuring the electron-impact RVE differential cross sections. They detected a manifold of resonance states, classified as series *a–d*. From the measured angular distributions they were able to identify the molecular symmetry of these states, while from the scattering data they were able to extract the corresponding potential curves and estimates of the resonance widths. The *a* series shows the most prominent peaks and is generated by the excited $^2\Sigma_g^+$ state of H_2^-. This state could also be responsible for the main peak at 14 eV in the experimental DEA cross sections. This aspect will be discussed in a future publication devoted to the dissociative attachment process [12]. We will focus here our attention on the vibrational excitation produced by the autodetachment of H_2^-, in the second excited $^2\Sigma_g^+$ resonant state, to the ground state of the H_2 molecule.

Calculations of potentials energies of H_2^- resonant states have been performed in the past at different levels of approximation [13]. In particular, an extensive study has been done by Stibbe and Tennyson (ST) [14–17], who have used the *R*-matrix method to calculate the potential curves and widths for a number of resonant states as a function of the internuclear separation, *R*. The existence of the excited $^2\Sigma_g^+$ symmetry state of H_2^- has been confirmed and the vibrational eigenvalues for this state have been calculated [17], in excellent agreement with the experimental values of Comer and Read [10].

The availability of this information on the excited resonant states of H_2^- opens the possibility for a theoretical study of the dynamics of RVE and DEA processes involving Rydberg states. At the same time, the calculated cross sections for these processes may be valuable in the modeling and diagnostics of low-temperature hydrogen plasmas [1,18]. In this paper we present a complete set of electron-impact differential cross sections for the resonant vibrational excitations of H_2, via the $^2\Sigma_g^+$ resonant state, in the collision energy range 11–14 eV where this process is effective.

In Sec. II we shall give a brief account of the electron-molecule resonant collision theory, while the computational details and results are presented in Secs. III and IV, respectively. In Sec. V we give our conclusions.

II. THEORETICAL MODEL

In briefly describing the electron-molecule resonant collision theory, and in particular its local complex-potential (LCP) approximation used in the present work, we shall follow the Refs. [19–21], to which the reader is referred to for more details.

*r.celiberto@poliba.it
†r.janev@fz-juelich.de
‡wadehra@wayne.edu
§annarita.laricchiuta@ba.imip.cnr.it

Let us denote by $\Phi_d(q,\mathbf{R}) \approx \phi_d(q;R)\xi(\mathbf{R})$ the wave function for the discrete state of the H_2^- ion expressed, in the Born-Oppenheimer approximation, as a product of the antisymmetric discrete electronic wave function ϕ_d, depending parametrically on the internuclear distance R, and the corresponding nuclear part $\xi(\mathbf{R})$. Here q collectively denotes the position coordinates of the $N+1$ electrons. The discrete states can overlap with the continuum spectrum of the H_2+e system, described by wave functions of the form $\Phi_\epsilon(q,R) \approx \psi_\epsilon(q;R)\chi_{vJ}(\mathbf{R})$, where ϵ is the projectile energy and v and J are the rovibrational quantum numbers of the target molecule. The complete wave function can then be expressed in terms of configuration interaction as [22]

$$\Psi = \Phi_d(q,\mathbf{R}) + \sum_{v,J} \int_0^\infty d\epsilon f_{v,J}(\epsilon)\Phi_\epsilon(q,\mathbf{R}), \tag{1}$$

where $f_{v,J}(\epsilon)$ are the expansion coefficients and the sum runs over all the accessible rovibrational states, including the continuum. The function $\psi_\epsilon(q;R)$ fulfills the outgoing wave boundary conditions except in the incident channel. The Schrødinger equation for the whole system is thus

$$H\Psi = [T_N + H_{el}(q,R)]\Psi = E\Psi, \tag{2}$$

where T_N is the nuclear kinetic energy operator and E is the total energy. The electronic Hamiltonian is defined as

$$H_{el}(q,R) = H_{el}^t + T_e + V_{et}(q), \tag{3}$$

where H_{el}^t is the target electronic Hamiltonian, T_e and V_{et} are, respectively, the projectile kinetic energy operator and the interaction potential with the target electrons. Inserting Eq. (1) in the Schrødinger equation a nonlocal integrodifferential equation is obtained for the nuclear wave function $\xi(\mathbf{R})$,

$$[T_N(\mathbf{R}) + V^-(R) - E]\xi(\mathbf{R}) = -V(\epsilon_i,R)\chi_{v_i,J_i}(\mathbf{R}) - \int d\mathbf{R}' K(\mathbf{R},\mathbf{R}')\xi(\mathbf{R}'), \tag{4}$$

where $V^-(R)$ is the H_2^- discrete state potential energy, and ϵ_i is the incident electron energy. The kernel of the integral on the right-hand side is given by

$$K(\mathbf{R},\mathbf{R}') = \sum_{v,J} \chi_{v,J}^*(\mathbf{R}')\chi_{v,J}(\mathbf{R})\left[\Delta(R',R,E-E_{v,J}) - \frac{i}{2}\Gamma(R',R,E-E_{v,J})\right], \tag{5}$$

where $E_{v,J}$ is the target rovibrational eigenvalue and the level shift Δ and the level width Γ have the nonlocal form

$$\Delta(R,R',\epsilon) = \mathrm{P}\int_0^\infty d\epsilon' \frac{V^*(\epsilon',R')V(\epsilon',R)}{\epsilon-\epsilon'} \tag{6}$$

and

$$\Gamma(R',R,\epsilon) = 2\pi V^*(\epsilon,R')V(\epsilon,R), \tag{7}$$

where P indicates the integral principal value. Both these quantities are defined in terms of *interaction matrix element* $V(\epsilon,R)$ between the discrete state and the continuum states,

$$V(\epsilon,R) = \int dq \phi_d^*(q;R)H_{el}(q,R)\psi_\epsilon(q;R). \tag{8}$$

In order to separate out the radial and the angular parts, we now write the two nuclear wave functions as

$$\xi(\mathbf{R}) = \sum_{J_r,m_r} \frac{\xi_{J_r,m_r}(R)}{R} Y_{J_r,m_r}(\hat{\mathbf{R}}) \tag{9}$$

and

$$\chi_{v,J}(\mathbf{R}) = \sum_m \frac{\chi_{v,J}(R)}{R} Y_{J,m}(\hat{\mathbf{R}}), \tag{10}$$

which, once inserted in Eq. (4), lead, after angular integration, to the radial equation

$$\left[-\frac{\hbar^2}{2M}\frac{d^2}{dR^2} + \frac{\hbar^2 J(J+1)}{2MR^2} + V^-(R) - E\right]\xi_i(R) = -V(\epsilon_i,R)\chi_{v_i,J}(R) - \int_0^\infty dR' K_J(R,R')\xi_i(R'), \tag{11}$$

where we have written J for J_i and m for m_i (no rotational transitions) and set $\xi_{J_i m_i} = \xi_i$. M is the reduced mass of the nuclei. The kernel $K_J(R,R')$ is still given by Eq. (5), where the vibrational wave functions $\chi_{v,J}(\mathbf{R})$ are now formally replaced by their radial part $\chi_{v,J}(R)$, and the sum is extended only over the vibrational quantum number v. It is customary to factorize the matrix elements as

$$V(\epsilon,R) = f(\epsilon)F(R) \tag{12}$$

so that the radial Eq. (11) can be written as

$$\left[-\frac{\hbar^2}{2M}\frac{d^2}{dR^2} + \frac{\hbar^2 J(J+1)}{2MR^2} + V^-(R) - E\right]\xi_i(R) = -f(\epsilon_i)F(R)\chi_{v_i,J}(R) - \sum_v c_{vJ}F(R)\chi_{vJ}(R)\int_0^\infty dR' \chi_{vJ}^*(R')F^*(R')\xi_i(R'), \tag{13}$$

where the quantity c_{vJ} is a function of $\epsilon_{vJ} = E - E_{vJ}$ defined by

$$c_{vJ} = \mathrm{P}\int_0^\infty d\epsilon \frac{|f(\epsilon)|^2}{\epsilon_{vJ}-\epsilon} - i\pi|f(\epsilon_{vJ})|^2. \tag{14}$$

The solution of Eq. (13) can be obtained by using the Green's function technique. Transforming the radial equation in integral form, and denoting the Green's function by $G(R,R')$, we get

$$\xi_i(R) = \int_0^\infty dR' G(R,R')F(R') \times \left[-f(\epsilon_i)\chi_{v_i,J}(R') - \sum_v c_{vJ}D_v\chi_{vJ}(R')\right]. \tag{15}$$

The integrals D_v are given by

$$D_v = \int_0^\infty dR \chi_{vJ}^*(R) F^*(R) \xi_i(R). \tag{16}$$

The D_v can be calculated by solving the matrix equation obtained by substituting, for ξ_i, from Eq. (15) into Eq. (16)

$$\sum_{v'} G_{vv'} D_{v'} = s_v, \tag{17}$$

where the coefficients $G_{vv'}$ and the inhomogeneous term s_v are given by

$$G_{vv'} = c_{v'J} \int_0^\infty dR \int_0^\infty dR' \chi_{vJ}^*(R) F^*(R) G(R,R') F(R') \chi_{v'J}(R') + \delta_{vv'}, \tag{18}$$

$$s_v = -f(\epsilon_i) \int_0^\infty dR \int_0^\infty dR' \chi_{vJ}^*(R) F^*(R) G(R,R') F(R') \chi_{v_iJ}(R'). \tag{19}$$

Once D_v are obtained, $\xi_i(R)$ can be finally found from Eq. (15).

The local form of the resonance model can be derived by imposing that the quantity c_{vJ} be independent of v and then using the completeness relation for the vibrational wave functions. This can be accomplished by replacing $\epsilon_{vJ}=E-E_{v,J}$ either by the incident electron energy $\epsilon_i=E-E_{v_i,J}$ or, alternatively, by the local energy $V^-(R)-V_0(R)$ which classically represents the kinetic energy of the incident electron captured or ejected at the internuclear distance R [19,23]. If, however, the interaction matrix elements are independent of ϵ and only known as a function of R, $f(\epsilon)$ in Eq. (12) reduces to the unity. This is a reasonable assumption since $f(\epsilon)$ goes to zero both for ϵ approaching zero (Wigner threshold law) and for ϵ approaching to infinity, and $f(\epsilon)$ is finite only for a small interval of energy centered around the singularity ϵ_{vJ}. Furthermore, if the *local* level shift, $\Delta(R)$, corresponding to the principal value integral of Eq. (14), is included in $V^-(R)$, then this last equation becomes simply

$$c_{vJ} = -i\pi. \tag{20}$$

Once the resonant nuclear wave function is obtained, the cross section can be calculated in a straightforward manner. It can be shown [24,25] that the RVE differential cross section, averaged over the molecular orientations, can be factorized as a product of the total cross section $\sigma_{v_iv_f}^{res}(E)$ and an angular part $g_{\bar{l}}(\theta)$ depending on the scattering angle θ, i.e.,

$$\left(\frac{d\sigma^{res}}{d\Omega}\right)_{v_i \to v_f} = \sigma_{v_iv_f}^{res}(E) g_{\bar{l}}(\theta). \tag{21}$$

The explicit form of $g_{\bar{l}}(\theta)$ will be given in the next section. We should mention here that in the usual treatment of the partial wave expansion of the differential cross section, only the dominant term $\bar{l}$ is retained. The total resonant cross section can then be expressed in terms of the T-matrix element as [20]

$$\sigma_{v_iv_f}^{res}(E) = \frac{k_f}{k_i} \int d\Omega |T_{i\to f}^{res}|^2 = \frac{4m^2\pi^3}{\hbar^4} \frac{k_f}{k_i} \left| \int dR \chi_{v_fJ}^*(R) V_{\bar{l}}^*(k_f,R) \xi_i(R) \right|^2, \tag{22}$$

where k_f is the momentum of the ejected electron and the *momentum normalized* matrix element $V_{\bar{l}}(k_f,R)$ is defined as

$$V_{\bar{l}}(k_f,R) = \left(\frac{\hbar^2}{mk_f}\right)^{1/2} V_{\bar{l}}(\epsilon_f,R), \tag{23}$$

where $V_{\bar{l}}(\epsilon_f,R)$ is the $\bar{l}$th term in the partial wave expansion of Eq. (8).

III. COMPUTATIONAL DETAILS

The present calculations have been carried out using the local complex potential (LCP) model. In this approximation Eq. (13), together with Eq. (20), reduces to the simpler analytical form

$$\left[-\frac{\hbar^2}{2M}\frac{d^2}{dR^2} + \frac{\hbar^2 J(J+1)}{2MR^2} + V^-(R) + i\frac{\pi}{2}\Gamma(R) - E\right] \xi_i(R) = -F(R)\chi_{v_iJ}(R). \tag{24}$$

However, from a numerical point of view, we have resolved the more general Eq. (13) by using the Green's function technique outlined above [19] with $J=0$. In this last equation the quantity $F(R)$ has been expressed, from Eqs. (7) and (12), as

$$|V(\epsilon,R)|^2 = |f(\epsilon)F(R)|^2 = |F(R)|^2 = \frac{1}{2\pi}\Gamma(R), \tag{25}$$

where, as mentioned previously, $V(\epsilon,R)$ is taken to be independent of ϵ [$f(\epsilon)=1$]. $\Gamma(R)$ has been linearly interpolated from the data of Ref. [15], where it is reported in the range of internuclear distances $1.1 \le R \le 4.0$ a.u. only. Outside this range, $\Gamma(R)$ has been obtained by linear extrapolation of the first two available points for $R<1.1$ a.u., while for $R>4.0$ a.u. the following Gaussian-like expression has been used [26]:

$$\Gamma(R) = 1.1639 e^{-0.48176(R-1.9)^2}, \tag{26}$$

where the numerical coefficients have been obtained by fitting the last three $\Gamma(R)$ values calculated by ST [15]. However, alternative functions have been tested for $\Gamma(R)$ outside the calculated interval and the final RVE cross sections have been found practically insensitive to the different extrapolations. In this context, in order to get a quantitative idea about the dependence of the cross sections on the variation of the level width, we have recalculated the cross sections by increasing $\Gamma(R)$ in Eq. (26) by 10%. No significant change in the value of the cross section has been observed. For $v=1$, for instance, the peak value of the recalculated differential cross sections has been found to be 5.87633×10^{-19} cm^2/sr, to be compared with 5.87626×10^{-19} cm^2/sr of the correct value. Both the peaks occur at the same incident energy of

11.29 eV. A similar situation was found also for excitation of higher vibrational levels. For $v=10$, for example, the absolute maximum of the recalculated cross sections reaches the value of 0.065169×10^{-19} cm^2/sr, which is only 0.035% lower than the original value of 0.065192×10^{-19} cm^2/sr. Variations of similar amounts in the values of cross sections have been obtained for $v=1$ and 10 by varying $\Gamma(R)$ by the same amount, namely 10%, in the region $R<1.1$ a.u. The observed very weak dependence of the cross sections on $\Gamma(R)$ is due to the fact that the vibrational wave functions, for both the neutral and the resonant states, vanish rapidly in the asymptotic region. A similar quantitative analysis has been performed also by varying the resonant state potential energy in the extreme regions of internuclear distances (see the discussion later).

A somewhat more noticeable variation in the cross sections has been observed, however, by increasing $\Gamma(R)$ by 10% in the whole interval of internuclear distances in our calculations $[0.4<R(\text{a.u.})<20]$. For both $v=1$ and $v=10$ (see Sec. IV) a decrease has been observed in the main peaks for these transitions of 12% and 16%, respectively. On the other hand, the positions of the peaks and the general shapes of the cross sections, as a function of the incident energy, remain unchanged. We may summarize these results by concluding that the cross sections are practically insensitive to $\Gamma(R)$ outside the Franck-Condon region for a given level, while, inside the region, small changes in the width do not strongly affect the differential cross sections which suffer only slight variations, remaining, however, still within the experimental uncertainties. This insensitivity suggests that all the RVE cross sections presented here would not be significantly altered by small variations in various resonance parameters. In particular, any error in the resonance width of Ref. [15], arising from the neglect of multichannel electronic coupling, would not lead to RVE cross sections which are noticeably different from the ones reported here. This is also understandable since, for electron energies in the range 11–14 eV, the majority of the scattering channels are open for molecular hydrogen and the effect of closed channels is quite minimal.

$V(\epsilon_i,R)$ has been obtained from the partial widths $\Gamma_X(R)$ of Ref. [15]. This quantity describes the formation of the resonant state by capture of the incident electron by the ground $X\ ^1\Sigma_g^+$ electronic state of the neutral H_2 molecule. The matrix elements have been expressed as $V(\epsilon_i,R)=[\Gamma_X(R)/2\pi]^{1/2}$. Outside the calculated range we used two different extrapolations. For $R<1.1$ a.u. we adopted the Wigner's threshold law form for $\Gamma_X(R)$,

$$\Gamma_X(R)=C\left[2m\frac{V^-(R)-V_0(R)}{\hbar^2}\right]^{\bar{l}+1/2}, \tag{27}$$

where C has been determined by normalizing $\Gamma_X(R)$ to the value calculated in Ref. [15], namely, $\Gamma_X(R=1.1$ a.u.). The orbital quantum number $\bar{l}$ has been set equal to 2 according to the d-wave nature of the resonance (see below). On the other side of the interval, we exploited the fact that, for large R, $\Gamma_X(R)$ is a constant fraction of the total width, as seen in the data of ST. We have then assumed, for $R>4.0$ a.u., $\Gamma_X(R)=\Gamma(R)\times0.046$, where 0.046 is the branching ratio for $R\geq3.8$ a.u. [27]. $V_0(R)$ is the potential curve for the neutral ground electronic state of H_2 taken from Ref. [28]. Figure 1 shows the total width $\Gamma(R)$ and the partial widths $\Gamma_X(R)$ as a function of the internuclear separation. The extrapolated parts are indicated by the dashed lines, while the circles, connected by full lines, indicate the calculated points [15].

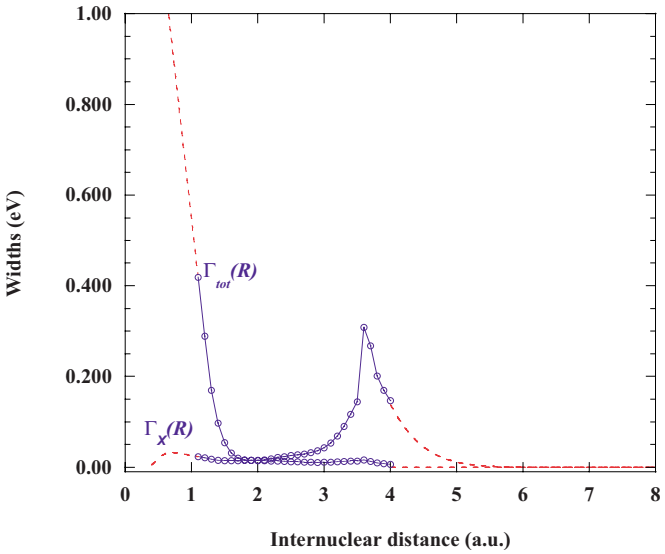

FIG. 1. (Color online) Total $\Gamma_{tot}(R)$ and partial $\Gamma_X(R)$ widths as a function of the internuclear distance R. Circles: calculated points [15] and dashed lines: extrapolated curves.

The potential energies $V^-(R)$ for the $^2\Sigma_g^+$ resonant state of the H_2^- molecular ion have been calculated by ST [15], again in the range $1.1\leq R\leq4.0$ a.u., using the R-matrix method. The theoretical curve reproduces quite well the corresponding potential energy function determined from experimental cross sections for the series a resonance [10,11]. The good agreement is also confirmed by the calculated vibrational eigenvalues which successfully compare with the vibrational energies obtained by other investigators [15,17]. In this context, it must be mentioned that Stibbe and Tennyson made a correction on their calculated vibrational energies of +0.08 eV, in order to take into account the inaccuracies in the parent state energies [15,17]. This correction is not implemented in the resonance positions (see page 821 and Table 18 in Ref. [15]) which are reported with respect to the ground electronic state energies of Table 2 of their paper. In the present work, in order to determine correctly the absolute positions of the resonance, we added to the resonant energies, for each bond length, the ground state energies as calculated by ST [15], and the above correction of +0.08 eV. The resulting potential has been checked by calculating the vibrational energy eigenvalues, $E_{v_rJ_r}$, of the resonant state, which were found in complete agreement with those of Ref. [15].

In the present work we used a cubic spline to interpolate the known potential energy data. Outside the calculated interval the following analytical expressions have been adopted to extend the potential function:

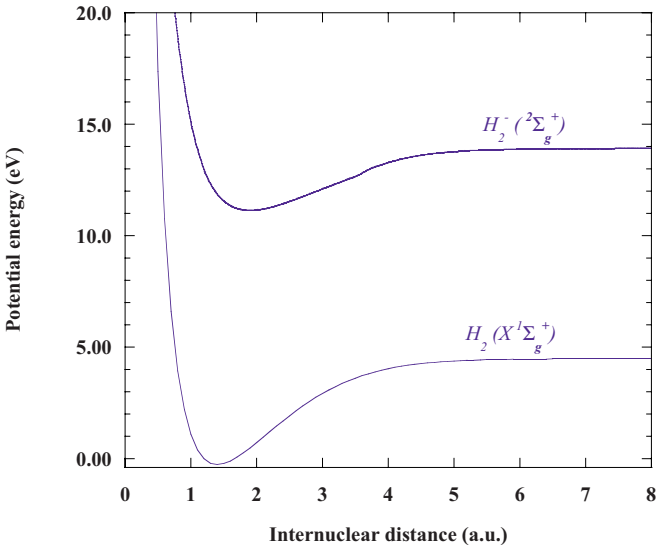

FIG. 2. (Color online) Potential energies curves as a function of the internuclear distance, R. Lower curve: neutral molecule ground electronic state. Upper curve: anion excited resonant state.

$$V^-(R < 1.1 \text{ a.u.}) = 71.34 - 123.55R + 97.253R^2 - 34.85R^3 + 4.7942R^4, \quad (28)$$

$$V^-(R > 4.0 \text{ a.u.}) = 13.9221 - \frac{1794.3}{R^6} + \frac{2196.9}{R^8} + \frac{2.7186 \times 10^5}{R^{10}} - 1052.8e^{-1.9143R}, \quad (29)$$

where the energies, in eV, are referred to the $v=0$ ground electronic state of a hydrogen molecule. The first function has been obtained by using a fourth-degree polynomial to interpolate the calculated data for $R<1.9$ a.u., while for $R>4.0$ a.u. we used a typical extrapolation constraining the function to the asymptotic energy of 13.9221 eV, corresponding to the atomic system $H(2s)+H^-(1s^2)$ [7]. In order to assess the sensitivity of the cross sections to the resonant potential curve in the far regions of the internuclear distances, where we have used the above extrapolations based on arbitrary functional forms, we have numerically studied the variation of cross sections by slightly altering the potential energy curves. We have then recalculated the cross sections for $v=1$ and $v=10$ after increasing the potential energy in Eq. (29) by 10%, just by changing the asymptotic constant from the value of 13.9221 to 15.3143. Comparing the obtained cross sections with those computed without any change in the potential energy curve, we found, for $v=1$, that the main peak value remained unchanged in the first five digits and no variations have been detected in its position, while for $v=10$ a reduction of the peak value of only 1.4% has been observed. A similar stability is shown by the $v=1$ cross sections recalculated after altering Eq. (28) by +10%, and for $v=10$ the reduction, around 0.39%, was even smaller than in the preceding case. In conclusion, the previous analysis, while showing that the choice of the extrapolation in the asymptotic regions of bond length is not crucial, confirms, at the same time, the weak dependence of the cross sections on the scattering parameters already discussed in this section.

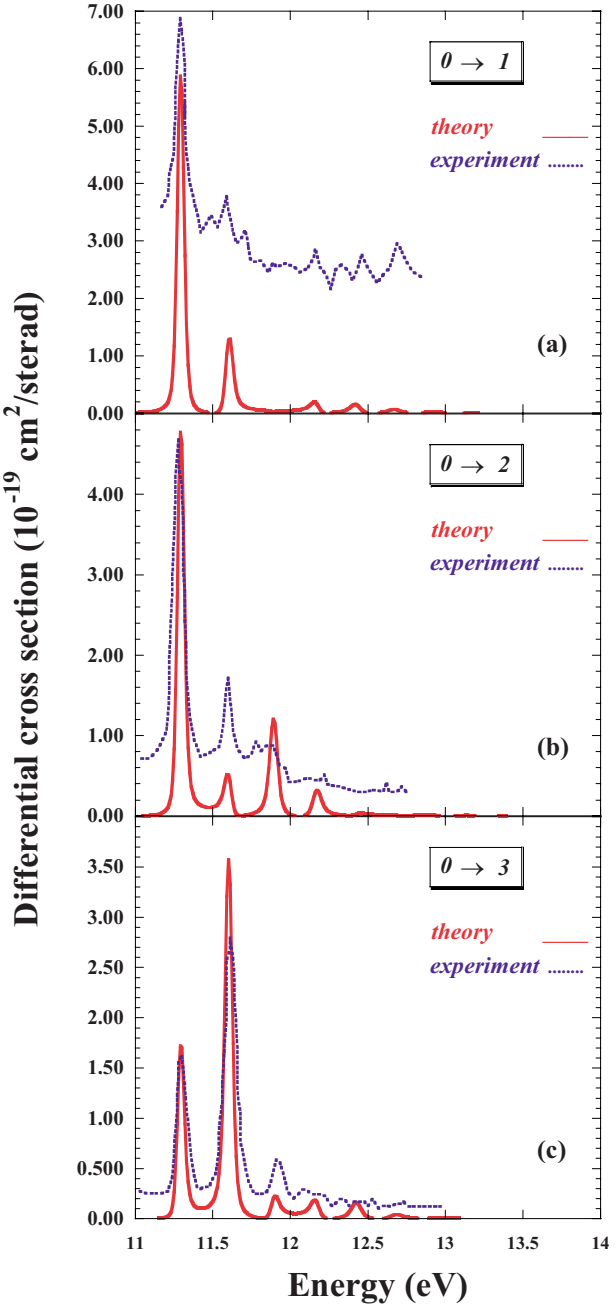

FIG. 3. (Color online) Cross section for the RVE process $v_i=0 \rightarrow v_f=1$, 2, and 3 for the scattering angle of 85°. Full curve: theoretical cross sections and dotted curve: measurements [10].

Figure 2 shows the final potential energy curve of the resonant state as a function of R, along with the target ground state energy $V_0(R)$. The angular factor $g_{\bar{l}}(\theta)$ in Eq. (21) can be written as [24,25]

$$g_{\bar{l}}(\theta) = \frac{1}{4\pi} \sum_{L=0}^{2\bar{l}} A_L P_L(\cos\theta), \quad (30)$$

where P_L is the Lth order Legendre polynomial, depending on the scattering angle θ, and A_L is given by

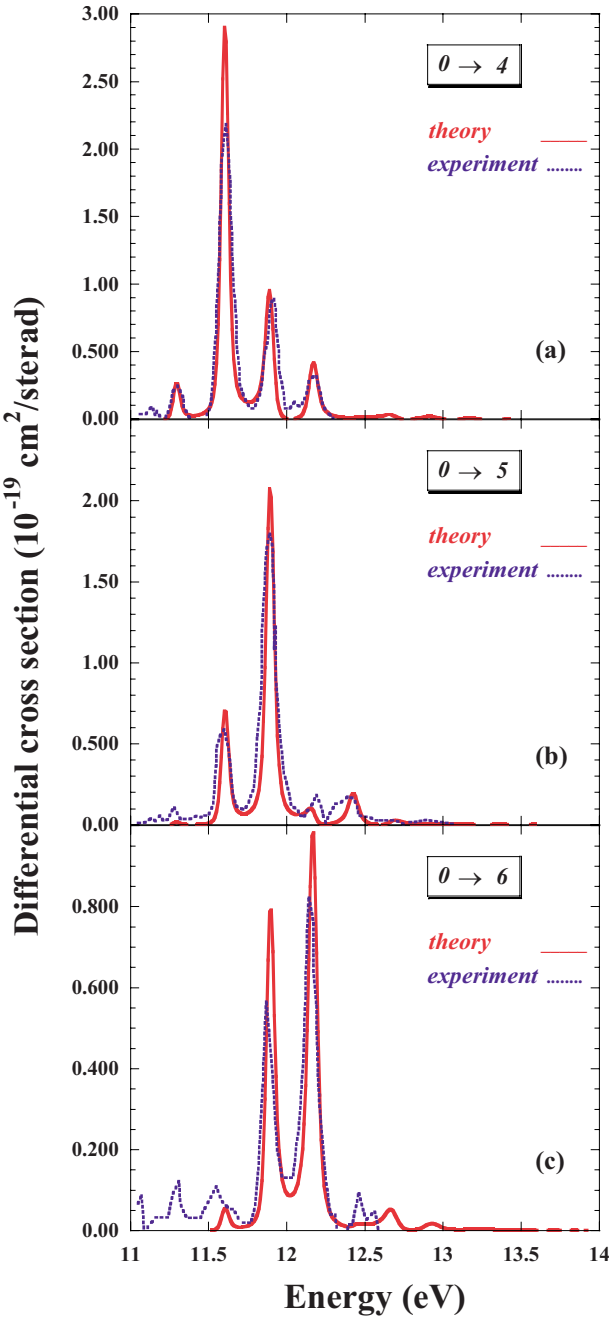

FIG. 4. (Color online) Same as Fig. 3 for v_f=4, 5, and 6.

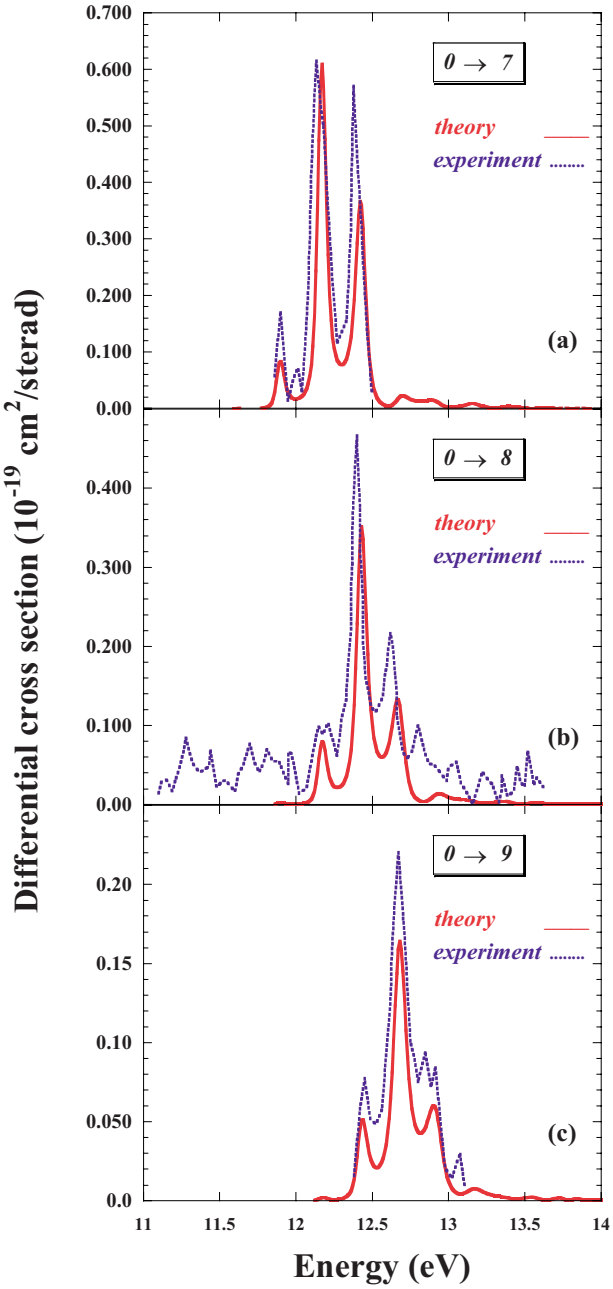

FIG. 5. (Color online) Same as Fig. 3 for v_f=7, 8, and 9.

$$A_L = (2\bar{l}+1)^2(2L+1)\sum_{m,m'}\begin{pmatrix} \bar{l} & \bar{l} & L \\ -m & m' & m'-m \end{pmatrix}^2 \times \begin{pmatrix} \bar{l} & \bar{l} & L \\ 0 & 0 & 0 \end{pmatrix}^2, \tag{31}$$

where the parentheses denote the usual 3-j symbols. The values of m and m' are determined by the symmetry of the resonant state. The angular factor $g_{\bar{l}}(\theta)$ is derived under the hypothesis that only one partial wave, selected by the nature of the resonant state, contributes to the resonant scattering. This assumption can be particularly appropriate for resonant Rydberg states, since, in this case, the molecular orbital where the incident electron is accommodated in the capturing process can show, to some extent, a pronounced atomic character, so that a single spherical harmonic can be sufficient to describe the angular part [29]. Therefore, according to the analysis of rotational excitations by electron impact of Joyez *et al.* [11], which established the $^2\Sigma_g^+$ symmetry for the series a resonance and estimated that the d wave gives the largest contribution to the scattering, we have assumed for the quantum numbers in Eqs. (30) and (31) the values $\bar{l}$=2 and m=m'=0. The final expression for $g_2(\theta)$ can then be written explicitly as

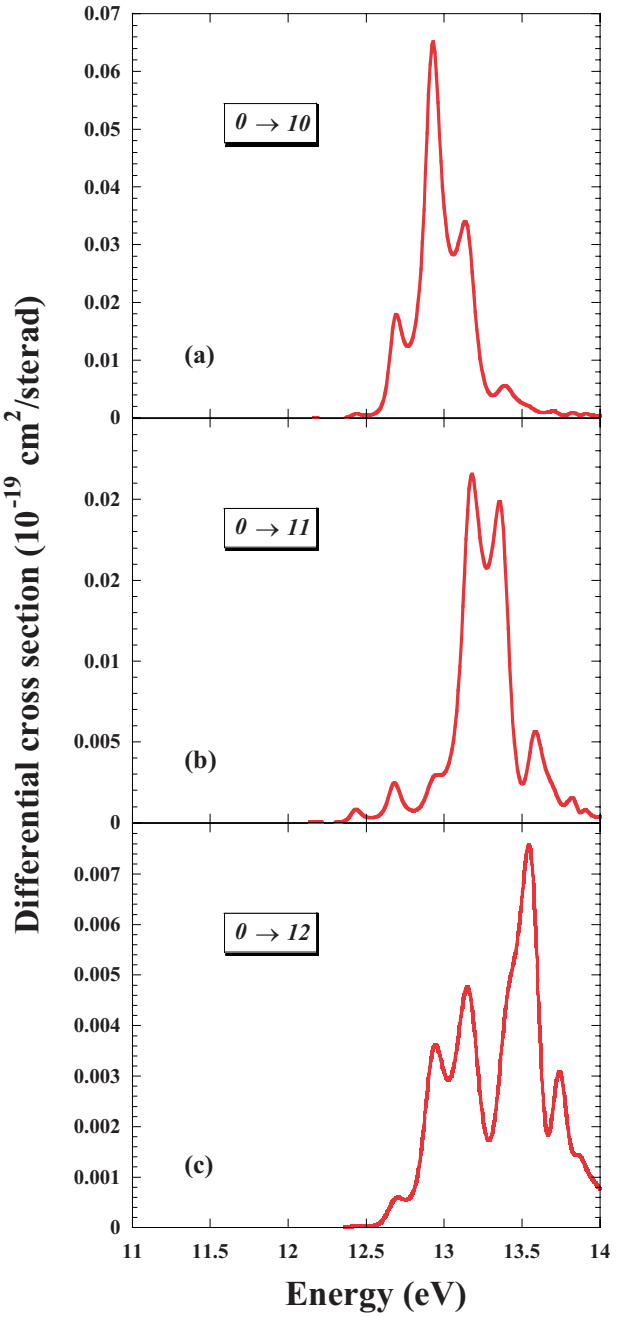

FIG. 6. (Color online) Same as Fig. 3 for v_f=10, 11, and 12. Only the theoretical cross section is shown (see text).

$$4\pi g_2(\theta) = \frac{15}{14}(1 - 2\cos^2\theta + 3\cos^4\theta). \quad (32)$$

The behavior of g_2 as a function of scattering angle is shown in Fig. 9.

IV. RESULTS

RVE differential cross sections have been calculated for the processes

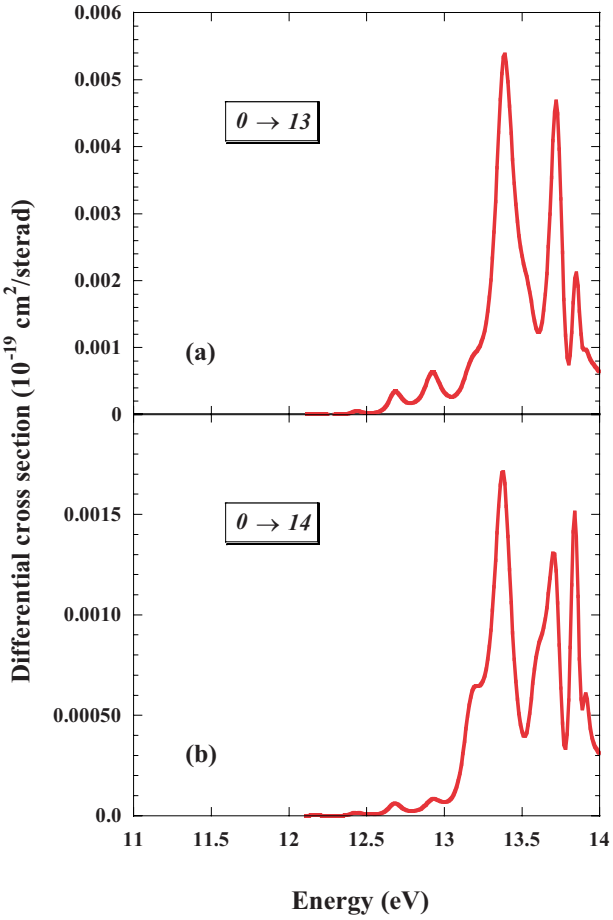

FIG. 7. (Color online) Same as Fig. 3 for v_f=13 and 14. Only the theoretical cross section is shown (see text).

$$H_2(X\,^1\Sigma_g^+, v_i = 0) + e \rightarrow H_2^{-*}(^2\Sigma_g^+) \rightarrow H_2(X\,^1\Sigma_g^+, v_f = 1 - 14) + e \quad (33)$$

starting from v_i=0 and ending on the excited vibrational levels v_f of the hydrogen molecule in the ground electronic state. In Figs. 3–5 a comparison between the experimental differential cross sections from Ref. [10], measured at the scattering angle of 85° for the exit channels v_f=1–9, and the present results is shown. The theoretical cross sections have been convoluted at the experimental resolution energy of 40 meV. In Fig. 3 it is evident that the background cross section due to the direct vibrational excitation, which is not considered in the present calculations, becomes rapidly negligible as v_f increases. For v_f=3 [Fig. 3(c)] it is remarkably reduced. In this case the theoretical cross sections exceed the experimental value at the main peak by a factor of about 1.2. This discrepancy is also present for v_f=4 in Fig. 4(a) and reduces for higher v_f, while for v_f=8 [Fig. 5(b)] the situation is reversed. The experimental cross sections, however, are correct to within about 20%, as reported by Comer and Read [10]. A further source of error comes from the fact that the experimental cross sections, shown in the figures, have been scanned from Fig. 3 of Ref. [10]. The spread of the data in fact made the acquisition of the points difficult, due to the overlap of many runs as explained by the authors. For v_f

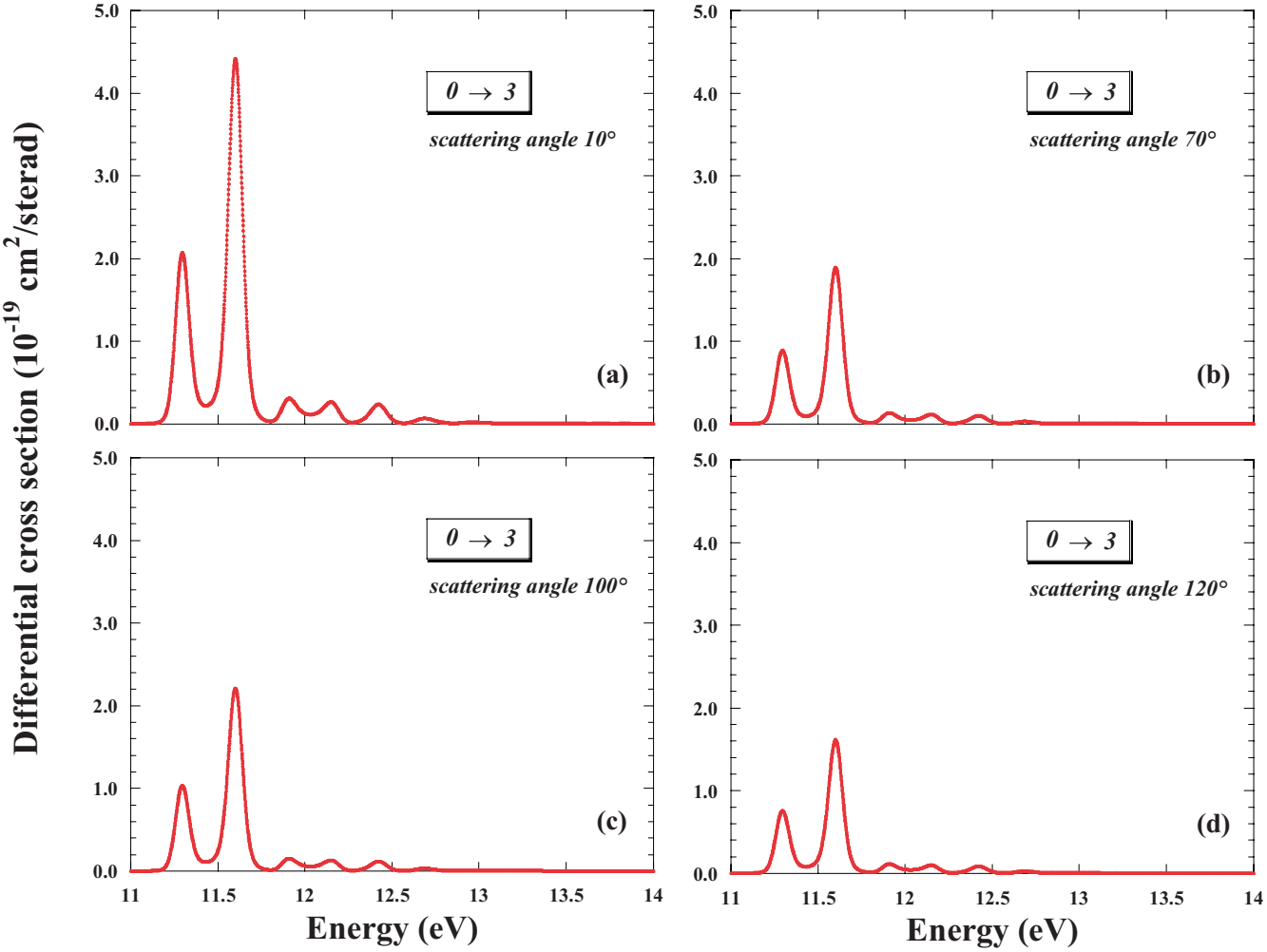

FIG. 8. (Color online) Differential cross section for the RVE transition $v_i=0\rightarrow v_f=3$ as a function of the scattering angle θ: (a) $\theta=10°$, (b) $\theta=70°$, (c) $\theta=100°$, and (d) $\theta=120°$.

$=10$ and 11, for example, we judged that the scanned values were meaningless and we omitted them in Figs. 6(a) and 6(b). In Figs. 6(c) and 7 finally, are shown the cross sections for $v_f=12-14$. For $v_f>11$ no experimental data are available.

The positions of the peaks in the cross sections are generally well-reproduced in all the figures. Some small differences are present for $v_f=8$ or 9, which, however, do not exceed the limit of the instrumental resolution. The well-separated and narrow peaks in Figs. 3, 4(a), and 4(b) ($v_f=1-5$) imply the validity of the compound-molecule limit ($\Gamma \ll \hbar\omega$). On the other hand, for the higher vibrational levels the enlargement and the overlap of the peaks, present in both the theoretical and experimental cross sections, can be interpreted as a sort of shift toward the impulse limit, probably due to the increase of the width $\Gamma(R)$ in the extreme regions of the internuclear distances, where the high-level vibrational wave functions reach their maximum, and to a simultaneous reduction of the eigenvalue spacing [30,31].

In order to check the angular behavior of vibrational excitation, we also calculated the cross sections at different scattering angles of 10°, 70°, 100°, and 120° for the exit channel $v_f=3$, for which measurements have been performed by Weingartshofer *et al.* [9]. Figures 8(a)–8(d) show the theoretical cross sections as a function of the energy. In order to facilitate a quick comparison of differential cross sections, all four frames in Fig. 8 are drawn with the same scale. Since in the present formulation the cross section is factorized in terms of an energy-dependent term and the angular factor $g_{\bar{l}}(\theta)$ [Eq. (21)], the shape of the differential cross sections remains unchanged for different angles. However, only the absolute peak values of the cross sections are affected by the angular factor, while their relative ratio remains constant. This is not in agreement with the experimental cross sections of Ref. [9] that show a progressive enhancement of the first maximum which becomes the main peak as the scattering angle approaches 120°. This behavior is attributed by the authors to interference of the resonant scattering with the direct scattering which, although small, is actually not negligible for $v_f=3$ [see also Fig. 3(c)]. A comparison between the measured cross sections [9] and the present calculations, for the $v_i=0\rightarrow v_f=3$ transition, as a function of the scattering angle, is shown in Fig. 9 for a fixed energy of 11.60 eV. The agreement is particularly satisfactory for large scattering angles, while some discrepancy arises at 10°, probably due to interference effects, which, however, does not exceed a factor of 1.5. In the same figure is shown also the angular factor,

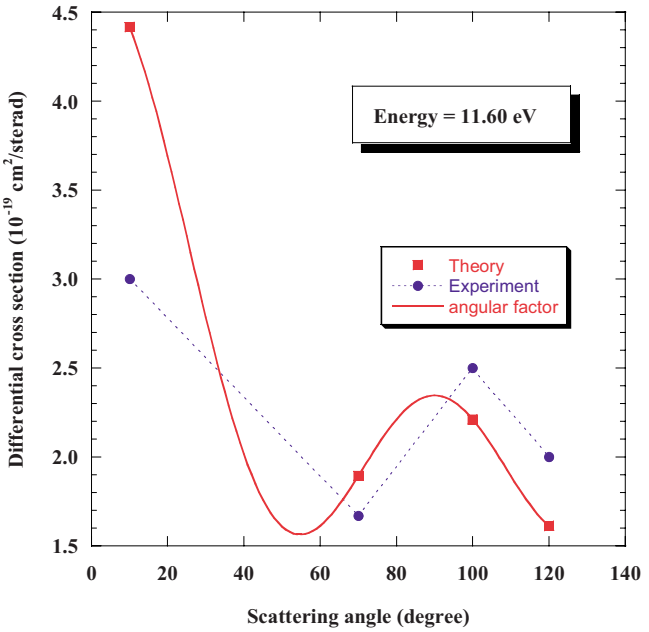

FIG. 9. (Color online) Experimental [9] (circles) and theoretical (squares) differential cross sections for the RVE transition $v_i=0 \rightarrow v_f=3$ for a fixed incident energy of 11.60 eV. The full line represents the angular factor $g_{\bar{l}=2}(\theta)$ [Eq. (32)] normalized to the first theoretical point.

$g_2(\theta)$ of Eq. (32), normalized to the first calculated point, which, at least for large angles, closely follows the experimental data.

The Feshbach nature of the resonant state is the basis for the good performance of the LCP model in reproducing the experimental cross sections. The long-lived resonances, in fact, are caused by a weak coupling between the discrete and continuum interaction which, through the coupling matrix element $V(\epsilon,R)$, determines a small width which is expected to have a weak dependence on the electron energy. A second aspect is represented by the large separation between the potential energy curves of the target molecule and of the resonant state (Fig. 2), which prevents the scattering process from threshold effects and, due to the large incident energies ($\epsilon_i \geq E_{v_f J_f} - E_{v_i J}$) involved in the collision, allows one to consider the vibrational channels as degenerate ($E_{vJ} \approx E_{v_i J}$). All these circumstances meet the main assumptions of the LCP model. The transition from the nonlocal complex potential model to the local one, in fact, can be implemented by the substitution of the final electron energy $\epsilon_f = E - E_{vJ}$ with the incident energy ϵ_i, which is valid for large kinetics energies and comparably small vibrational spacing of the target molecule. This assumption, however, retains some dependence of the coupling matrix elements on the incident energy. The complete suppression of this dependence in the present calculations, coming from the fact that the width is available as a function of the bond length only, is less trivial and is justified *a posteriori* by the good agreement between theory and experiment.

V. CONCLUSIONS

We have calculated the electron-impact RVE cross sections associated with the excited $^2\Sigma_g^+$ resonant Rydberg state of the hydrogen molecule. The real and the imaginary parts of the potential energy of the discrete anion state were taken from *ab initio* calculations reported in the literature [15] and appropriately extrapolated. A complete set of $v_i=0 \rightarrow v_f$ ($v_f=1-14$) RVE cross sections has been calculated in the incident electron energy range of 11–14 eV. The calculations have been performed in the frame of the local complex potential approximation and a satisfactory agreement with the available experimental cross sections is obtained. The observed agreement can be interpreted as due to the favorable peculiarities of the scattering system that satisfy the main assumptions of the LCP model and, thus, allow for a realistic description of the collision process without the introduction of any empirical or adjustable parameters.

ACKNOWLEDGMENTS

This work has been partially supported by MIUR PRIN 2005 (Grant No. 2005039049_005). The authors are indebted to Dr. D. Pagano and Dr. I. Cadez for useful discussions and suggestions.

[1] M. Capitelli and C. Gorse, IEEE Trans. Plasma Sci. IEEE Nucl. Plasma Sci. Soc. **33**, 1832 (2005).
[2] G. J. Schulz, Rev. Mod. Phys. **45**, 423 (1973).
[3] I. I. Fabrikant, J. M. Wadehra, and Y. Xu, Phys. Scr. **T96**, 45 (2002).
[4] J. Horáček, M. Čížek, K. Houfek, P. Kolorenč, and W. Domcke, Phys. Rev. A **73**, 022701 (2006), and references therein.
[5] G. J. Schulz, Phys. Rev. **113**, 816 (1959).
[6] D. Rapp, T. E. Sharp, and D. D. Briglia, Phys. Rev. Lett. **14**, 533 (1965).
[7] T. E. Sharp, At. Data **2**, 119 (1971).
[8] C. E. Kuyatt, S. R. Mielczarek, and J. A. Simpson, Phys. Rev. Lett. **12**, 293 (1964); C. E. Kuyatt, J. A. Simpson, and S. N. Mielczarek, J. Chem. Phys. **44**, 437 (1966); D. E. Golden and H. W. Bandel, Phys. Rev. Lett. **14**, 1010 (1965); D. E. Golden, H. W. Bandel, and I. A. Salerno, Phys. Rev. **146**, 40 (1966); M. G. Menendez and H. K. Holt, J. Chem. Phys. **45**, 2743 (1966).
[9] A. Weingartshofer, H. Ehrhardt, V. Herman, and F. Linder, Phys. Rev. A **2**, 294 (1970).
[10] J. Comer and F. H. Read, J. Phys. B **4**, 368 (1971).
[11] G. Joyez, J. Comer, and F. H. Read, J. Phys. B **6**, 2427 (1973).
[12] Paper in preparation.
[13] H. S. Taylor and J. K. Williams, J. Chem. Phys. **42**, 4063 (1965); I. Eliezer, H. S. Taylor, and J. K. Williams, *ibid.* **47**, 2165 (1967).
[14] D. T. Stibbe and J. Tennyson, J. Phys. B **29**, 4267 (1996).
[15] D. T. Stibbe and J. Tennyson, J. Phys. B **31**, 815 (1998).

[16] D. T. Stibbe and J. Tennyson, J. Phys. B **30**, L301 (1997).
[17] D. T. Stibbe and J. Tennyson, Phys. Rev. Lett. **79**, 4116 (1997).
[18] S. Markelj, Z. Rupnik, and I. Cadez, *Proceedings of the 27th International Conference on Phenomena in Ionized Gases*, Eindhoven, The Netherlands, July 18–22, 2005), p. 2–236 and p. 8–237.
[19] D. E. Atems and J. M. Wadehra, Phys. Rev. A **42**, 5201 (1990).
[20] J. M. Wadehra, in *Non equilibrium Vibrational Kinetics*, edited by M. Capitelli, Topics in Current Physics Vol. 39 (Springer-Verlag, Berlin, 1986), p. 191.
[21] A. U. Hazi, T. N. Rescigno, and M. Kurilla, Phys. Rev. A **23**, 1089 (1981).
[22] J. N. Bardsley, J. Phys B (Proc. Phys. Soc.) **1**, 349 (1968).
[23] J. N. Bardsley, in *Electron-Molecule and Photon-Molecule Collisions*, edited by T. Rescigno, V. McKoy, and B. Schneider (Plenum, New York, 1979).
[24] L. Dubé and A. Herzenberg, Phys. Rev. A **20**, 194 (1979).
[25] E. S. Chang, Phys. Rev. A **16**, 1841 (1977).
[26] C. Mundel, M. Berman, and W. Domcke, Phys. Rev. A **32**, 181 (1985).
[27] See Table 4 in Ref. [15].
[28] W. Kolos and L. Wolniewicz, J. Chem. Phys. **43**, 2429 (1965).
[29] R. I. Hall and F. H. Read, in *Electron-Molecule Collisions*, edited by I. Shimamura and K. Takayanagi (Plenum Press, New York, 1984), p. 351.
[30] J. N. Bardsley and F. Mandl, Rep. Prog. Phys. **31**, 471 (1968).
[31] See, for example, Fig. 3 and Table 5 in Ref. [15].